A Novel Post-Processing Method for Nonlinearity Correction of FMCW LiDAR

Yi Hao, Yaqi Han, Connie Chang-Hasnain and H. Y. Fu*
Tsinghua Shenzhen International Graduate School,
Tsinghua University,
Shenzhen, China
*E-mail: hyfu@sz.tsinghua.edu.cn

***Abstract*—A novel post-processing nonlinearity correction method for the FMCW LiDAR system without the assistance of an auxiliary interferometer is presented. The optimized energy diffusion and the enhanced ranging resolution are experimentally validated.**

Keywords—FMCW LiDAR, nonlinearity correction, post-processing

I. INTRODUCTION

Frequency-modulated continuous-wave (FMCW) light detection and ranging (LiDAR) is a promising three-dimensional ranging technique in scientific and high-tech industrial applications. Because of the large frequency bandwidth in the optical domain and the coherent detection scheme, FMCW LiDAR can achieve higher ranging resolution and much better sensitivity and robustness against environmental disturbances compared with the LiDAR based on the time-of-flight (TOF) scheme [1]. However, when the modulation is applied to the optical frequency of laser, the relationship between the laser wavelength and injection current is normally nonlinear, and the temperature of the gain medium is affected by the current as well, which results in the wavelength fluctuation and thus the nonlinearity of laser frequency sweep [2]. Consequently, the frequency of the beat signal is no longer a constant, as well as the spectrum is broadened and the energy is diffused following the Fourier transform. These phenomena will eventually reduce the ranging resolution and accuracy. Correcting the nonlinearity is essential to improve the ranging performance in the FMCW LiDAR system.

Various available correction approaches have been proposed to address this issue. A closed-loop correction approach adopting an electronic-photonic phase-locked loop (PLL) is directly added on a tunable laser to produce a negative feedback loop and locks the frequency of the beat signal in an interferometer to a clean electronic local oscillator for compensating the frequency sweep rate of the laser [3]. Another correction approach based on a pre-distorted technique concentrates on generating a linear pre-distorted laser drive voltage waveform with different iterative methods, such as iterative learning control [4] and zero-crossing [5]. Besides, these two approaches are also combined to precisely control the linear frequency sweep in [6]. These approaches are capable of outputting swept light with high linearity and are independent of the specific lasers, but still have drawbacks. On the one hand, the electronic structure with a short loop delay in the PLL increases the complexity of the system and the susceptibility to external interference. On the other hand, the optimal scale factor for the pre-distortion technique depends on the lasers, demanding numerous times of trial-and-error to ensure the convergence speed and the least residual nonlinearity.

Apart from the aforementioned hardware-based approaches, the nonlinearity correction can also be accomplished by the commonly-used resampling method introducing an auxiliary interferometer to acquire a reference beat signal serving as a resampling clock. By means of the reference signal, the measured beat signal will be resampled in an equal optical frequency interval thereby compensating the nonlinearity in the data acquisition time interval [7], [8]. While the resampling method reduces the system complexity to a certain extent, the maximum range of detection is confined by the delayed length of the auxiliary interferometer to satisfy the Nyquist-Shannon sampling theorem [9]. To avoid the restrictions, the Hilbert transform is adopted to extract the nonlinear component of the frequency sweep from the auxiliary interferometer and the nonlinearity is then compensated. However, this method requires a phase unwrapping procedure [10].

Herein, regarding the phase of the nonlinearity term in the beat signal as a polynomial expression, a post-processing nonlinearity correction method named improved high-order ambiguity function and discrete match Fourier transform (IHAF-DMFT) is proposed. The nonlinearity coefficients of the discrete beat signal acquired from the FMCW LiDAR system are estimated firstly based on the improved high-order ambiguity function (IHAF) method. Afterwards, the nonlinearity term in the beat signal is normalized and transformed into a novel time function as the path of integration in the Fourier transform. This method is free of the redundant auxiliary interferometer, as well as the requirement of phase unwrapping. A Monte-Carlo simulation and ranging experiments based on a tunable vertical-cavity surface-emitting laser (VCSEL) are conducted to verify the superior performance of the proposed method in nonlinearity correction for FMCW LiDAR.

II. NONLINEARITY ANALYSIS AND CORRECTION METHOD

In light of the Stone-Weierstrass theorem and Anghel et al. [11], the phase of the nonlinearity term can be generally approximated by an *M*-order polynomial function. When the target is close to FMCW LiDAR, i.e., the round-trip time delay τ is sufficiently small compared with the frequency sweep period, the phase of the beat signal can be written as

$$\varphi_b(t) = 2\pi\tau \sum_{m=0}^{M} \alpha_m t^m , \tag{1}$$

where α_m is the m th-order nonlinearity coefficient, $\alpha_0 = f_0 - 1/2\gamma\tau$, $\alpha_1 = \gamma$, f_0 is the optical carrier frequency, γ is the linear frequency sweep rate of laser (in Hz/s), $\gamma\tau$ denotes the frequency of the beat signal.

When a range profile is calculated by the Fourier transform of the beat signal, each nonlinearity coefficient in (1) will diffuse the energy and aggravate the ranging resolution. Consequently, a correction method named IHAF-DMFT is proposed to estimate the nonlinearity coefficients with the IHAF and eliminate the nonlinearity coefficients by discrete match Fourier transform (DMFT).

A. Estimation of the Nonlinearity Coefficients

To obtain the well-estimated nonlinearity coefficients, researchers have proposed a dozen different kinds of methods [9], [12]. One of the most favorable methods is the high-order ambiguity function (HAF), which has the similar capability of detecting harmonic signals by the Fourier transform [13]. Compared with other nonlinearity correction methods, the HAF directly extracts the nonlinearity coefficients from the beat signal without the requirement of phase unwrapping.

In this method, the frequency f_m of each ambiguity function has a corresponding relationship with the nonlinearity coefficient, which satisfies

$$f_m = m!\left(\tau_{HAF}\Delta t_s\right)^{m-1}\alpha_m , \tag{2}$$

where τ_{HAF} is the delay parameter of the HAF, Δt_s is the sampling interval. Herein, f_m is generally calculated by the Fourier transform. Regarding this result, M-order nonlinearity coefficients can be estimated by an iterative procedure of the HAF summarized in [13].

Nevertheless, the inevitable picket fence effect influences the measured accuracy of f_m, which will eventually result in estimation with low accuracy of these nonlinearity coefficients. Therefore, a spectrum correction method with chirp z-transform (CZT) is introduced to improve the performance of the HAF.

Employing the process described in [14], an optimized spectrum of each ambiguity function will be acquired. Afterwards, The m th-order estimated nonlinearity coefficients can be computed by

$$\hat{\alpha}_m = \frac{\hat{f}_m}{m!\left(\tau_{HAF}\Delta t_s\right)^{m-1}\tau} , \tag{3}$$

where $\hat{f}_m$ is the optimized frequency of each ambiguity function, $m = 1,2\ldots,M$.

B. Elimination of the Nonlinearity Coefficients

Normalizing the nonlinearity term with $\hat{\alpha}_1$, the beat signal can be represented as

$$s_b(t) = \exp\left\{j2\pi\tau\left[f_0 - 1/2\gamma\tau + \hat{\alpha}_1\xi(t)\right]\right\} , \tag{4}$$

which becomes a linear function with respect to $\xi(t)$, $\xi(t) = t + \sum_{m=2}^{M}\hat{\alpha}_m t^m / \hat{\alpha}_1$.

It can be easily proved the derivative of $\xi(t)$ is continuous as well as $\xi(0) = 0$, which meets the requirements of the statement in [15]. Computing the spectrum of the beat signal regarding $\xi(t)$ as the new path of integration will focus the energy of the beat signal on the main lobe, thus eliminating the nonlinearity coefficients. In practice, this integration path is target range independent, since $\hat{\alpha}_m$ is normalized by $\hat{\alpha}_1$. The rough value of τ will be only required when determining the choice of τ_{HAF} by comparing the value of $\hat{\alpha}_1$ and γ.

Consequently, the spectrum of the discrete beat signal $s_b(n)$, i.e., the equation of DMFT can be written as

$$\begin{aligned} S_b(p) = \frac{1}{N}\sum_{n=0}^{N-1} s_b(n)\exp\left[-j2\pi p\delta f\xi(n\Delta t_s)\right] \\ \times\left\{\xi(n\Delta t_s) - \xi\left[(n-1)\Delta t_s\right]\right\} \end{aligned} , \tag{5}$$

where $\delta f = 1/\xi(N\Delta t_s)$ is the frequency resolution of $S_b(p)$.

III. Experimental Results and Discussions

This section mainly contains two parts: A Monte-Carlo simulation on the estimation performance of the nonlinearity coefficients and ranging experiments on the nonlinearity correction performance with a tunable VCSEL in an FMCW LiDAR system.

A. Simulation of the Estimation Method

To verify the IHAF, a transmitted signal with a nonlinearity of 4.81% was simulated, whose linear frequency sweep rate of laser was 5 THz/s. After a round-trip time delay by a target located at 0.7 m, a beat signal was generated and sampled with a sampling interval of 2 µs. The phase of nonlinearity term in the simulation was assigned as $2\pi\tau\left(3t^2 + 10t^3 + 5t^4 + 13t^5\right)\times 10^{12}$.

The Monte-Carlo simulation was conducted by estimating the nonlinearity coefficients with the IHAF and the HAF from the sampled beat signals, whose signal-to-noise ratios (SNRs) varied from 0 dB to 50 dB. Herein, an evaluation parameter named Mean Squared Error (MSE in dB) is introduced to indicate the performance of the estimation method, which indicates the extent of deviation between the estimated values and the actual value. The MSE of $\hat{\alpha}_m$ by L times Monte-Carlo simulation can be represented as

$$MSE_m = 10\lg\left[\frac{1}{L}\sum_{l=1}^{L}\left(\hat{\alpha}_{m,l} - \alpha_m\right)^2\right], \tag{6}$$

where $\hat{\alpha}_{m,l}$ is the l-th Monte-Carlo simulation results of $\hat{\alpha}_m$. The estimation results of 300 times Monte-Carlo simulation are plotted in Fig. 1.

For the beat signals with SNRs greater than or equal to 10 dB, the estimation error of the IHAF is much minor than the estimation error of the HAF. The reason is that the CZT efficiently improves the frequency resolution and reduces the influence of the picket fence effect, which indicates the value of f_m and thus the estimated nonlinearity coefficients are more accurate. However, the estimation performance of the IHAF deteriorates when the SNRs of the beat signals are less than 10dB, which is nearly the same as the estimation performance of the HAF. This indicates the substantial noise has a significant impact on the estimation of nonlinearity coefficients. On account of the results above, the IHAF-DMFT has great validity in obtaining the well-estimated nonlinearity coefficients.

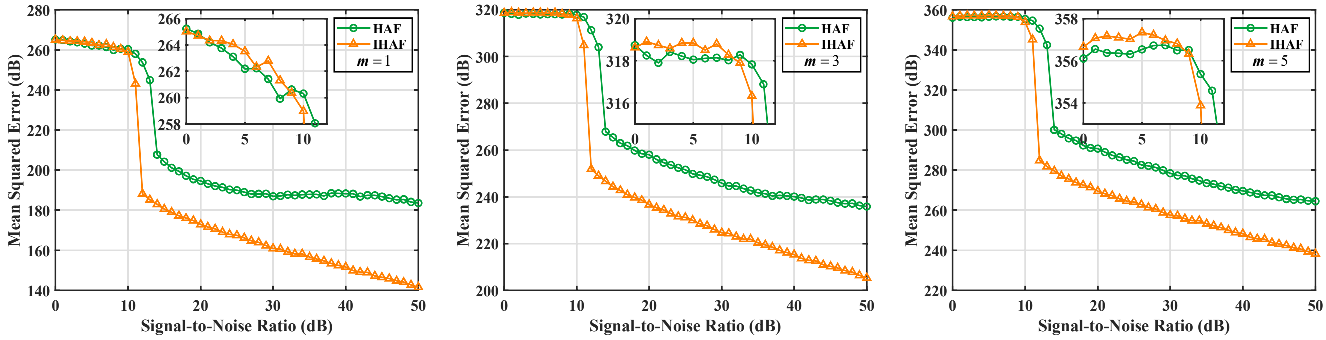

(a) (b) (c)

Fig. 1. Comparison between the IHAF and the HAF of 300 times Monte-Carlo simulation results for signals with SNRs from 0 dB to 50 dB. (a)–(c) represent the first, the third, and the fifth nonlinearity coefficient $\hat{\alpha}_m$, respectively.

B. Ranging Experiments of the Correction Method

Fig. 2 illustrates the experimental setup of the FMCW LiDAR system. A tunable VCSEL, with precise details in [16], is modulated by a triangular-wave voltage generated from an arbitrary function generator (AFG) with a modulated frequency of 10 kHz. A swept light of the VCSEL with a swept range from 1553.00 nm to 1561.07 nm is amplified by an Erbium-doped fiber amplifier (EDFA) and split into two parts with a 90/10 coupler. 90% of the light is routed by a circulator and used to obtain the round-trip time delay between a collimator and the target, regarded as the received signal. 10% of the light is considered as the local signal with the same phase as the transmitted signal. After coherent detection by a 50/50 coupler and a balanced photodetector (BPD), the beat signal is generated. By virtue of a high-speed oscilloscope, the beat signal can be sampled with a sampling interval of 0.8 ns and used for signal processing.

In the ranging experiments, a highly reflective metal block as the target was placed at 0.76 m in front of the FMCW LiDAR system. By processing the sampled beat signal in one frequency sweep period, the time-frequency curve can be acquired. As shown in Fig. 3, the frequency of the beat signal is increasing with time rather than a constant, indicating a significant nonlinearity of laser frequency sweep with VCSEL. Since the impact of unsatisfactory mixing at the up and down-sweep end, 80% of the up-sweep, as the red region in Fig. 3, was selected for the nonlinearity correction.

After the time-frequency transform, the range profiles of the target with and without nonlinearity correction are plotted in Fig. 4. Owing to the influence of nonlinearity, the energy of the spectrum without correction is diffused severely. Consequently, the main lobe is shifted to 0.69 m and the full width at half maximum (FWHM) is 0.52 mm. In other words, the nonlinearity leads to a wrong measurement of target distance and a deteriorated ranging resolution. To prove the validity of the IHAF-DMFT, the traditional resampling method using an auxiliary interferometer of fibers was compared as well. In Fig. 4(b), the beat signal was resampled in equal intervals of frequency, whose ranging resolution has a slight enhancement. Nevertheless, a side lobe with almost the same amplitude still exists, interfering the measurement of target distance. With the nonlinearity correction by the IHAF-DMFT, as illustrated in Fig. 4(c), the range profile has one explicit main lobe and the FWHM is only 0.36 mm, which means this method is capable of optimizing energy diffusion and improving the ranging resolution. The results of the ranging experiments demonstrate the superior performance of the proposed method in nonlinearity correction. In addition, the proposed method has no requirement for the auxiliary interferometer compared with the traditional resampling

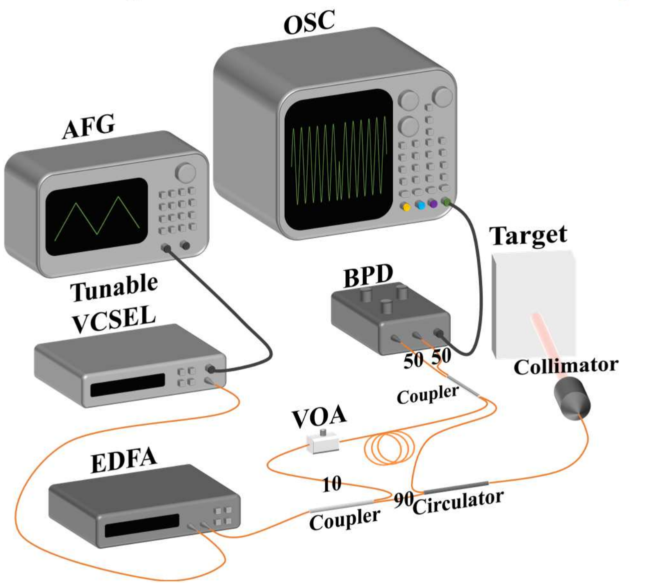

Fig. 2. The schematic of the FMCW LiDAR system. AFG: arbitrary function generator; EDFA: Erbium-doped fiber amplifier; VOA: variable optical attenuator; BPD: balanced photodetector; OSC: oscilloscope.

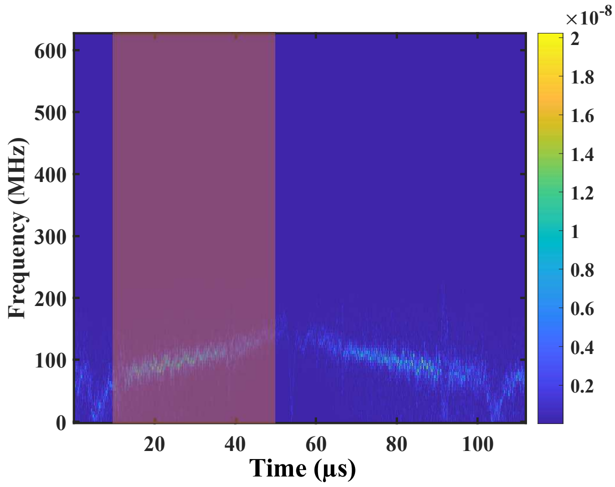

Fig. 3. The time-frequency curve of the sampled beat signal in one frequency sweep period. The red region represents the region of nonlinearity correction.

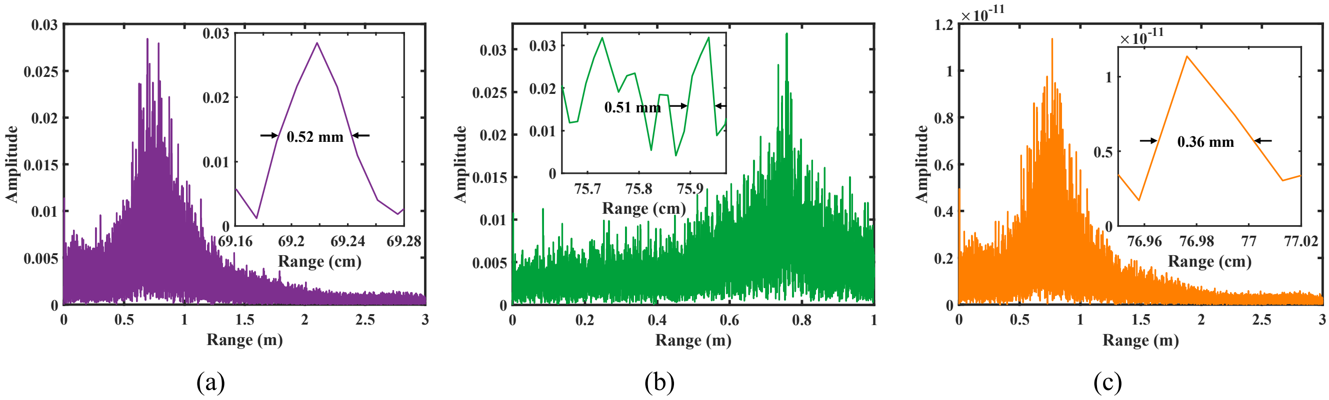

Fig. 4. Range profiles and full width at half maximum (FWHM) of the target (a) without correction and corrected by different methods: (b) traditional resampling method using an auxiliary interferometer of fibers and (c) IHAF-DMFT method.

method, which significantly minimizes the complexity of the FMCW LiDAR system.

IV. Conclusion

A novel post-processing nonlinearity correction method for the FMCW LiDAR system is proposed. Based on the HAF method, the IHAF-DMFT estimates the nonlinearity coefficients by measuring the frequency of each ambiguity function with optimized frequency resolution. Then a new time function consisting of these estimated coefficients by normalizing is regarded as the path of integration in the Fourier transform. The simulation results indicate the proposed method can obtain the well-estimated nonlinearity coefficients. The capability of optimizing energy diffusion and improving the ranging resolution with the IHAF-DMFT are also demonstrated by the comparison results with the traditional resampling method in the FMCW LiDAR experiments. The proposed method has superior performance in nonlinearity correction and low system complexity for FMCW LiDAR.

Acknowledgment

The authors would like to express sincere thanks to the Shenzhen Technology and Innovation Council (WDZC20200820160650001).

References

[1] B. Behroozpour, P. A. M. Sandborn, M. C. Wu, and B. E. Boser, “Lidar system architectures and circuits,” IEEE Commun. Mag., vol. 55, no. 10, pp. 135–142, October 2017.

[2] L. Jia, Y. Wang, X. Wang, F. Zhang, W. Wang, J. Wang, and et al., “Nonlinear calibration of frequency modulated continuous wave LIDAR based on a microresonator soliton comb,” Opt. Lett., vol. 46, no. 5, pp. 1025–1028, March 2021.

[3] B. Behroozpou, P. A. M. Sandborn, N. Quack, T. Seok, Y. Matsui, M. C. Wu, et al., “Electronic-photonic integrated circuit for 3D microimaging,” IEEE J. Solid-State Circuit, vol. 52, no. 1, pp. 161–172, January 2017.

[4] X. Zhang, J. Pouls, and M. C. Wu, “Laser frequency sweep linearization by iterative learning pre-distortion for FMCW LiDAR,” Opt. Express, vol. 27, no. 7, pp. 9965–9974, April 2019.

[5] P. Li, Y. Zhang, and J. Yao, “Rapid linear frequency swept frequency-modulated continuous wave laser source using iterative pre-distortion algorithm,” Remote Sens., vol. 14, no. 14, pp. 3455, July 2022.

[6] N. Satyan, A. Vasilyev, G. Rakuljic, V. Leyva, and A. Yariv, “Precise control of broadband frequency chirps using optoelectronic feedback,” Opt. Express, vol. 17, no. 18, pp. 15991–15999, August 2009.

[7] P. A. M. Sandborn, T. Hariyama, and M. C. Wu, “Resolution-enhancement for wide-range non-Linear FMCW lidar using quasi-synchronous resampling,” in Imaging and Applied Optics, 2017, pp. DW3F.3.

[8] C. Li, F. Zhang, and X. Qu, “High-resolution frequency-modulated continuous-wave LiDAR using multiple laser sources simultaneously scanning,” J. Lightwave Technol., vol. 41, no. 1, pp. 367–373, January 2023.

[9] R. Wang, M. Xiang, B. Wang, and C. Li, “Nonlinear phase estimation and compensation for FMCW ladar based on synchrosqueezing wavelet transform,” IEEE Geosci. Remote Sens. Lett., vol. 18, no. 7, pp. 1174–1178, July 2021.

[10] T. Ahn, J. Y. Lee, and D. Y. Kim, “Suppression of nonlinear frequency sweep in an optical frequency-domain reflectometer by use of Hilbert transformation,” Appl. Opt., vol. 44, no. 35, pp. 7630–7634, December 2005.

[11] A. Anghel, G. Vasile, R. Cacoveanu, C. Ioana, and S. Ciochina, “Short-range wideband FMCW radar for millimetric displacement measurements,” IEEE Trans. Geosci. Remote Sensing, vol. 52, no. 9, pp. 5633–5642, September 2014.

[12] S. Bai, X. Zhou, L. Zhang, H. Wang, and J. Yuan, “Nonlinear correction of frequency-modulated continuous-wave lidar frequency modulation based on singular value decomposition-least square algorithm,” Opt. Eng., vol. 59, no. 5, pp. 056106, May 2020.

[13] S. Peleg and B. Friedlander, “The discrete polynomial-phase transform,” IEEE Trans. Signal Process., vol. 43, no. 8, pp. 1901–1914, August 1995.

[14] L. R. Rabiner, R. W. Schafer, and C. M. Rader, “The chirp z-transform algorithm,” IEEE Trans. Audio Electroacoust., vol. AU-17, no. 2, pp. 86–92, June 1969.

[15] S. Wang, S. Li, J. Ni, and G. Zhang, “A new transform—Match Fourier transform,” Acta Electronica Sinica, vol. 29, no. 3, pp. 403–405, March 2001.

[16] Y. Han, Z. Li, L. Wu, S. Mai, X. Xing, and H. Y. Fu, “High-speed two-dimensional spectral-scanning coherent LiDAR system based on tunable VCSEL,” J. Lightwave Technol., vol. 41, no. 2, pp. 412–419, January 2023.